

Multiple functional variants in the *IL1RL1* region are pretransplant markers for risk of GVHD and infection deaths

Ezgi Karaesmen,¹ Theresa Hahn,² Alexander James Dile,³ Abbas A. Rizvi,¹ Junke Wang,¹ Tao Wang,^{4,5} Michael D. Haagenson,⁶ Leah Preus,¹ Qianqian Zhu,⁷ Qian Liu,⁷ Li Yan,⁷ Song Liu,⁷ Christopher A. Haiman,⁸ Daniel Stram,⁸ Loreall Pooler,⁸ Xin Sheng,⁸ David Van Den Berg,⁸ Guy Brock,⁹ Amy Webb,⁹ Philip L. McCarthy,² Marcelo C. Pasquini,⁴ Stephen R. Spellman,⁶ Stephanie J. Lee,¹⁰ Sophie Paczesny,^{3,*} and Lara E. Sucheston-Campbell^{1,11,*}

¹Division of Pharmaceutics and Pharmacology, College of Pharmacy, The Ohio State University, Columbus, OH; ²Department of Medicine, Roswell Park Comprehensive Cancer Center, Buffalo, NY; ³Department of Pediatrics, Indiana University School of Medicine, Indianapolis, IN; ⁴Center for International Blood and Marrow Transplant Research, Department of Medicine, Medical College of Wisconsin, Milwaukee, WI; ⁵Division of Biostatistics, Institute for Health and Society, Medical College of Wisconsin, Milwaukee, WI; ⁶Center for International Blood and Marrow Transplant Research, Minneapolis, MN; ⁷Department of Biostatistics, Roswell Park Comprehensive Cancer Center, Buffalo, NY; ⁸Department of Preventive Medicine, University of Southern California, Los Angeles, CA; ⁹Department of Biomedical Informatics, The Ohio State University, Columbus, OH; ¹⁰Clinical Research Division, Fred Hutchinson Cancer Research Center, Seattle, WA; and ¹¹Department of Veterinary Biosciences, College of Veterinary Medicine, The Ohio State University, Columbus, OH

Key Points

- Multiple functional variants in 2q12.1 region, containing *IL1RL1*, are strongly associated with sST2 levels, a well-characterized GVHD biomarker.
- Donor variants in the 2q12.1 region associated with sST2 also associate with death from infection or aGVHD.

Graft-versus-host disease (GVHD) and infections are the 2 main causes of death without relapse after allogeneic hematopoietic cell transplantation (HCT). Elevated soluble serum stimulation-2 (sST2), the product of *IL1RL1* in plasma/serum post-HCT, is a validated GVHD biomarker. Hundreds of SNPs at 2q12.1 have been shown to be strongly associated with sST2 concentrations in healthy populations. We therefore hypothesized that the donor genetic variants in *IL1RL1* correlate with sST2 protein levels associated with patient survival outcomes after HCT. We used DISCOVeRY-BMT (Determining the Influence of Susceptibility Conveying Variants Related to 1-Year Mortality after Blood and Marrow Transplantation), a genomic study of >3000 donor-recipient pairs, to inform our hypothesis. We first measured pre-HCT plasma/serum sST2 levels in a subset of DISCOVeRY-BMT donors ($n = 757$) and tested the association of donor sST2 levels with donor single nucleotide polymorphisms (SNPs) in the 2q12.1 region. Donor SNPs associated with sST2 levels were then tested for association with recipient death caused by acute GVHD (aGVHD), infection, and transplant-related mortality in cohorts 1 and 2. Meta-analyses of cohorts 1 and 2 were performed using fixed-effects inverse variance weighting, and P values were corrected for multiple comparisons. Donor risk alleles in rs22441131 ($P_{\text{meta}} = .00026$) and rs2310241 ($P_{\text{meta}} = .00033$) increased the cumulative incidence of aGVHD death up to fourfold and were associated with high sST2 levels. Donor risk alleles at rs4851601 ($P_{\text{meta}} = 9.7 \times 10^{-7}$), rs13019803 ($P_{\text{meta}} = 8.9 \times 10^{-6}$), and rs13015714 ($P_{\text{meta}} = 5.3 \times 10^{-4}$) increased cumulative incidence of infection death to almost sevenfold and were associated with low sST2 levels. These functional variants are biomarkers of infection or aGVHD death and could facilitate donor selection, prophylaxis, and a conditioning regimen to reduce post-HCT mortality.

Introduction

Approximately 30 000 allogeneic hematopoietic cell transplantations (HCTs) were performed worldwide in 2018. Graft-versus-host disease (GVHD) and infections are the 2 main causes of nonrelapse mortality after HCT. Elevated soluble serum stimulation-2 (sST2) levels in patients after

transplantation is a validated biomarker of therapy-resistant GVHD and death.¹⁻⁸ The ST2 protein is encoded by the *IL1RL1* gene, which is located on chromosome 2 (chr 2; 2q12) and produces 2 isoforms: soluble or circulating (sST2) and membrane-bound or cellular (ST2).⁹ The membrane-bound isoform (ST2) induces immune response through its only ligand, interleukin-33 (IL-33), and promotes MyD88/NF- κ B signaling, whereas the soluble isoform (sST2) lacks transmembrane and cytoplasmic domains, does not signal, and acts as a decoy receptor, sequestering free IL-33 in serum.^{9,10} ST2 is a member of the IL-1 receptor family, and the ST2/IL-33 pathway has been implicated in several immune and inflammatory diseases, as well as cardiovascular events.^{9,10}

In 5 independent genome-wide association studies (GWASs) totaling tens of thousands of healthy individuals, multiple single nucleotide polymorphisms (SNPs) within a 1-megabase (Mb) region around *IL1RL1* (chr 2; 102.5-103.5 Mb) associated with sST2 protein levels at the genome-wide significance level $P < 5 \times 10^{-8}$.¹¹⁻¹⁶ There are additional genomic features that make this an appealing region to search for biomarkers of aGVHD and infection death. Specifically, variants in this 1-Mb span correlate significantly with gene expression levels of *IL1RL1* and other *IL1* family members in healthy blood, lung, skin, and esophageal tissues.^{13,17-19} Analyses of the human primary blood cell type Promoter Capture Hi-C (PCHi-C) data attempt to link gene regulatory elements to their target genes and show that this region contains over 1000 promoter-interaction regions (PIRs).²⁰⁻²² PIRs in lymphoblastoid cell lines are significantly enriched for autoimmune GWAS SNPs.^{23,24} In line with this finding, the 1-Mb region surrounding *IL1RL1* contains >70 unique genome-wide significant SNPs associated with multiple infection or immune-related phenotypes, asthma, Crohn's disease, ulcerative colitis (UC), celiac disease, ankylosing spondylitis,^{15,25-27} inflammatory bowel disease (IBD), percentages of neutrophils, and percentage and counts of eosinophils and lymphocytes.²⁸ Together, these data provide a strong rationale for testing the association of SNPs in this region with recipient survival after HCT.

We sought to determine whether variants in the *IL1RL1* region are associated with sST2 levels in DISCOVeRY-BMT (Determining the Influence of Susceptibility Conveying Variants Related to 1-Year Mortality after Blood and Marrow Transplantation) recipients and donors and in turn whether these sST2-associated variants increase the risk of death from aGVHD, from infection, and from transplantation-related events. Evidence of a genetic association suggests that these may be functional survival biomarkers and could be used to improve donor selection and to better understand the biological complexity of death due to aGVHD or infection.

Patients and methods

Study population

The study population consisted of the 2 cohorts comprising DISCOVeRY-BMT, an existing well-powered genome-wide association study (GWAS) totaling 3047 HCT recipients who were of European genomic ancestry and had acute lymphoblastic leukemia (ALL), acute myelogenous leukemia (AML), or myelodysplastic syndrome (MDS), and their HLA-matched unrelated

donors, treated from 2000 through 2011 and reported to the Center for International Blood and Marrow Transplant Research (CIBMTR).²⁹⁻³² All patients included in DISCOVeRY-BMT provided informed consent for inclusion in the CIBMTR registry and biorepository. Paired donor and recipient biospecimens and corresponding clinical data were obtained from the CIBMTR biorepository and database. The National Marrow Donor Program (NMDP), Roswell Park Comprehensive Cancer Institute, The Ohio State University, and Indiana University School of Medicine Institutional Review Boards approved the study protocol. In this study, we focused on patients with AML or MDS and their donors ($n = 2253$ pairs) in DISCOVeRY-BMT. We defined aGVHD death and infection death as primary nonoverlapping causes of death in the absence of disease relapse, with secondary causes defined as contributing, because these were either not as severe as the primary cause or were more distal from the time of death.²⁹

Genotyping and imputation

Genotyping and quality control have been described in detail.²⁹⁻³² In brief, samples were randomized to plates³³ and genotyped by using the Illumina Human OmniExpress BeadChip (University of Southern California Genomics Facility). After sample quality control, 2111 (cohort 1) and 777 (cohort 2) donor-recipient pairs of European genomic ancestry were available for analyses. Following SNP QC, ~635 000 SNPs were imputed to the hg19 build 37 Haplotype Reference Consortium (<http://www.haplotype-reference-consortium.org/home>). To make the population more homogenous, we included only myeloid samples (AML and MDS) from DISCOVeRY-BMT. Variants were analyzed if the minor allele frequency (MAF) was >0.05 and the info score was >0.8, yielding 2271 SNPs on chr 2 (102.5-103.5 Mb) in 1584 (cohort 1) and 669 (cohort 2) donor-recipient pairs.

Pre-HCT sST2 plasma and serum concentration measurements

A subset of DISCOVeRY-BMT AML and MDS samples with available plasma or serum were selected for pre-HCT sST2 measurement. In total, we measured sST2 levels in 1514 samples: 757 pretransplantation patients and their matched donors. Samples were collected before initiation of the preparative regimen for transplantation. This collection may have occurred before or on the day of admission. Enzyme-linked immunosorbent assays (ELISAs) for ST2 were performed in batches on cryopreserved plasma and serum.^{2,6-8} Approximately three-quarters of all samples measured were from plasma (treated with anticoagulant citrate dextrose) and the remaining one-fourth were from serum.

Statistical analyses

SNP associations with pre-HCT sST2 levels. SNPs were tested for association with plasma/serum sST2 concentrations by using linear regression models adjusted for age, sex, and sample type (plasma or serum) in a subset of DISCOVeRY-BMT donor-recipient pairs ($n = 757$). sST2 values were \log_{10} transformed for normalization. Donor and recipient SNPs were tested for association with donor and pretransplant recipient sST2 serum/plasma concentrations, respectively. Dosage SNP data (ranging from 0 to 2 alleles), accounting for the probability of each genotype, were used in all regression

Table 1. Characteristics of patients enrolled in the study

Category/characteristics	Cohort 1 (N = 1584), n (%)	Cohort 2 (N = 669), n (%)	Cohort with sST2 level measurements (N = 756), n (%)
Recipient age, y			
≥40	1132 (71)	481 (72)	532 (70)
<40	452 (29)	188 (28)	224 (30)
Donor age, y^a			
≥30	963 (61)	347 (52)	392 (52)
<30	621 (39)	322 (48)	364 (48)
Recipient sex			
Female	723 (46)	303 (45)	340 (45)
Male	861 (54)	366 (55)	416 (55)
Donor sex			
Female	498 (31)	181 (27)	198 (26)
Male	1086 (69)	488 (73)	558 (74)
Blood mismatch			
No type mismatch	674 (43)	293 (44)	332 (44)
Donor–recipient mismatch	910 (57)	376 (56)	424 (56)
Anti-thymocyte globulin/alemtuzumab prophylaxis*			
No	1074 (68)	396 (59)	477 (63)
Yes	407 (26)	273 (41)	277 (37)
Missing	103 (7)	0 (0)	2 (0.3)
Obese BMI			
No	1084 (68)	446 (67)	500 (66)
Yes	500 (32)	223 (33)	256 (34)
Overweight BMI			
No	1079 (68)	444 (66)	508 (67)
Yes	505 (32)	225 (34)	248 (33)
Graft type^a			
Bone marrow	505 (32)	161 (24)	260 (34)
Peripheral blood	1079 (68)	508 (76)	496 (66)
Conditioning intensity			
Myeloablative	1079 (68)	453 (68)	549 (73)
Reduced intensity	505 (32)	216 (32)	207 (27)
Total body irradiation			
No	1021 (64)	472 (71)	489 (65)
Yes	563 (36)	197 (29)	267 (35)
Disease status at diagnosis			
Early	1107 (70)	428 (64)	486 (64)
Advanced	477 (30)	241 (36)	270 (36)
Recipient CMV status			
Negative	716 (45)	306 (46)	361 (48)
Positive	868 (55)	363 (54)	395 (52)
Donor CMV status			
Negative	1080 (68)	472 (71)	513 (68)
Positive	504 (32)	197 (29)	243 (32)
Diagnosed with AML^a			
No	337 (21)	192 (29)	208 (28)
Yes	1247 (79)	477 (71)	548 (72)

Table 1. (continued)

Category/characteristics	Cohort 1 (N = 1584), n (%)	Cohort 2 (N = 669), n (%)	Cohort with sST2 level measurements (N = 756), n (%)
Diagnosed with MDS			
No	1247 (79)	477 (71)	548 (72)
Yes	337 (21)	192 (29)	208 (28)
Primary cause of death			
aGVHD	95 (0.06)	56 (0.08)	49 (0.06)
Infection	86 (0.05)	25 (0.04)	36 (0.05)

*Significant difference between cohorts 1 and 2 ($P < .001$).

models run in R statistical software.³⁴ Linkage disequilibrium (LD) between the SNPs and SNP annotation was visualized with the R package LDheatmap and SNIPA online tool, respectively.^{34,35}

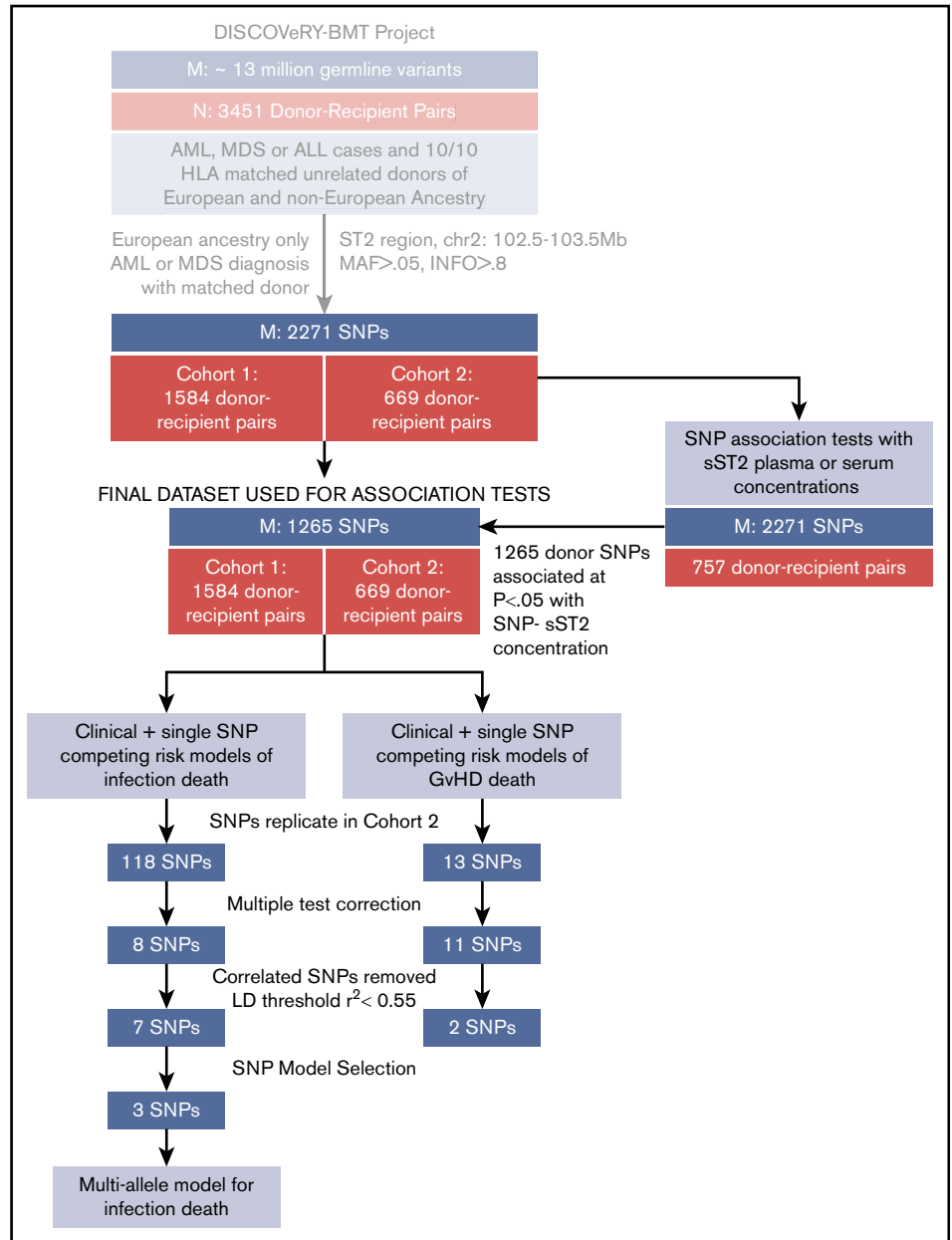
Competing risk analyses of aGVHD death and infection death.

Before genetic analyses, bidirectional stepwise competing risk models were constructed for both outcomes and run in the R package *crrstep*.^{34,36,37} Akaike information criteria (AIC) were used to select the best-fit clinical model in cohort 1. These variables were used for competing risk SNP analyses in both cohorts 1 and 2. The following variables were tested: recipient age <40, donor age, recipient sex, donor sex, anti-thymocyte globulin/alemtuzumab (Campath) prophylaxis, body mass index category, ABO blood group, conditioning intensity, graft source, total body irradiation AML (yes/no), disease stage, and CMV status. SNP meta-analyses were performed by fitting fixed-effects models with inverse variance weighting, using the R package Metafor. Random-effects models were used to provide meta-analyses estimates if heterogeneity was detected between cohorts, defined as Cochran's Q value > 50 or $P < .05$.³⁸ Bonferroni correction for the effective number of independent genetic tests, after adjusting for the correlation between tested SNPs, was used to determine significance.³⁹ A SNP association was deemed statically significant if the direction of hazard was the same in both cohorts and had a meta P (P_{meta}) < 5.3×10^{-4} . These significant SNPs were then also tested for association with overall survival (OS), using the Cox proportional hazards model, and transplant-related mortality (TRM), using the competing risk model, while adjusting for other clinical variables. To measure the collective contribution of significant variants to risk of death due to infection, a multiallele variable was generated, defined as the sum of the number of risk alleles across significantly associated SNPs selected in the models described above. This variable was then used in the final competing risk model with clinical covariates.

Annotation of significantly associated variants

We annotated significant SNPs in the *IL1RL1* region (chr 2; 102.5-103.5 Mb) using publicly available data to better understand the potential function of the variants identified. eQTLGen, a consortium analyses of the relationship of SNPs to gene expression in 30 912 whole blood samples, was used to determine if aGVHD or infection death-associated SNPs showed an allele-specific association with nearby gene expression

Figure 1. Study schema showing analytic workflow. The flow diagram shows the selection process for both the samples (N) and SNPs (M) for analyses of aGVHD and infection death in the DISCOVERy-BMT study.



(*cis*-expression quantitative trait loci [eQTL]). A catalog of human blood cell trait variation²⁸ and the genomic atlas of the human plasma proteome¹³ were used to determine if significant SNPs showed an allele-specific association with plasma protein levels in >3000 healthy individuals. Significant variants were also examined for relationship to gene expression in >70 additional tissues using the Genotype-Tissue Expression Project (GTEx; <https://gtexportal.org/home/>). To determine if our significant SNPs were associated with other traits or diseases, we queried the PhenoScanner database, a comprehensive variant-phenotype database of large GWASs, which includes results from the UK Biobank, NHGRI-EBI GWAS catalog, NIH GRASP, and publicly available summary statistics from >100 published genome association studies.¹⁹ Results were filtered at $P < 5 \times 10^{-8}$, and the R statistical software package PhenoScanner

(<https://github.com/phenoscanner/phenoscanner>) was used to download all data for our significant variants. Chromatin state data based on a 25-state Imputation Based Chromatin State Model across 24 blood, T-cell, hematopoietic stem cell (HSC), and B-cell lines were downloaded from the Roadmap Epigenomics project⁴⁰ Web site (<https://egg2.wustl.edu/roadmap/data/byFileType/chromhmmSegmentations/ChmmModels/imputed12marks/jointModel/final/>). Figures including chromatin state information and results from previous GWASs were constructed using the R Bioconductor package *gviz*.⁴¹ Last, publicly available PCHI-C data on a lymphoblastoid cell line (LCL), GM12878, were used to identify PIRs within our 1-Mb region.^{22,42} In brief, PCHI-C, uses Hi-C libraries with biotinylated RNA baits complementary to the ends of all promoter-containing restriction fragments to enrich for promoter sequences. The promoters and the genome pieces

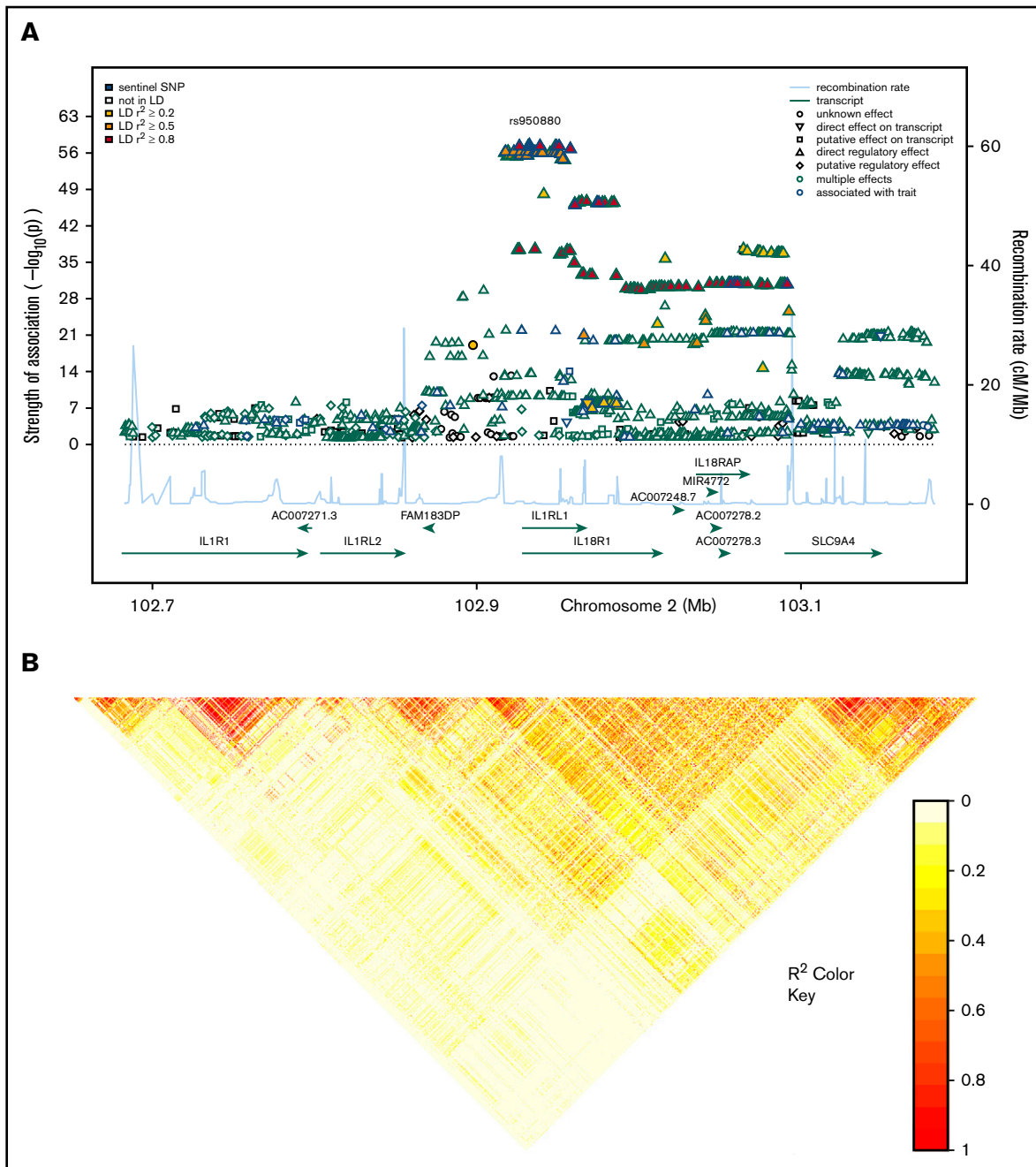


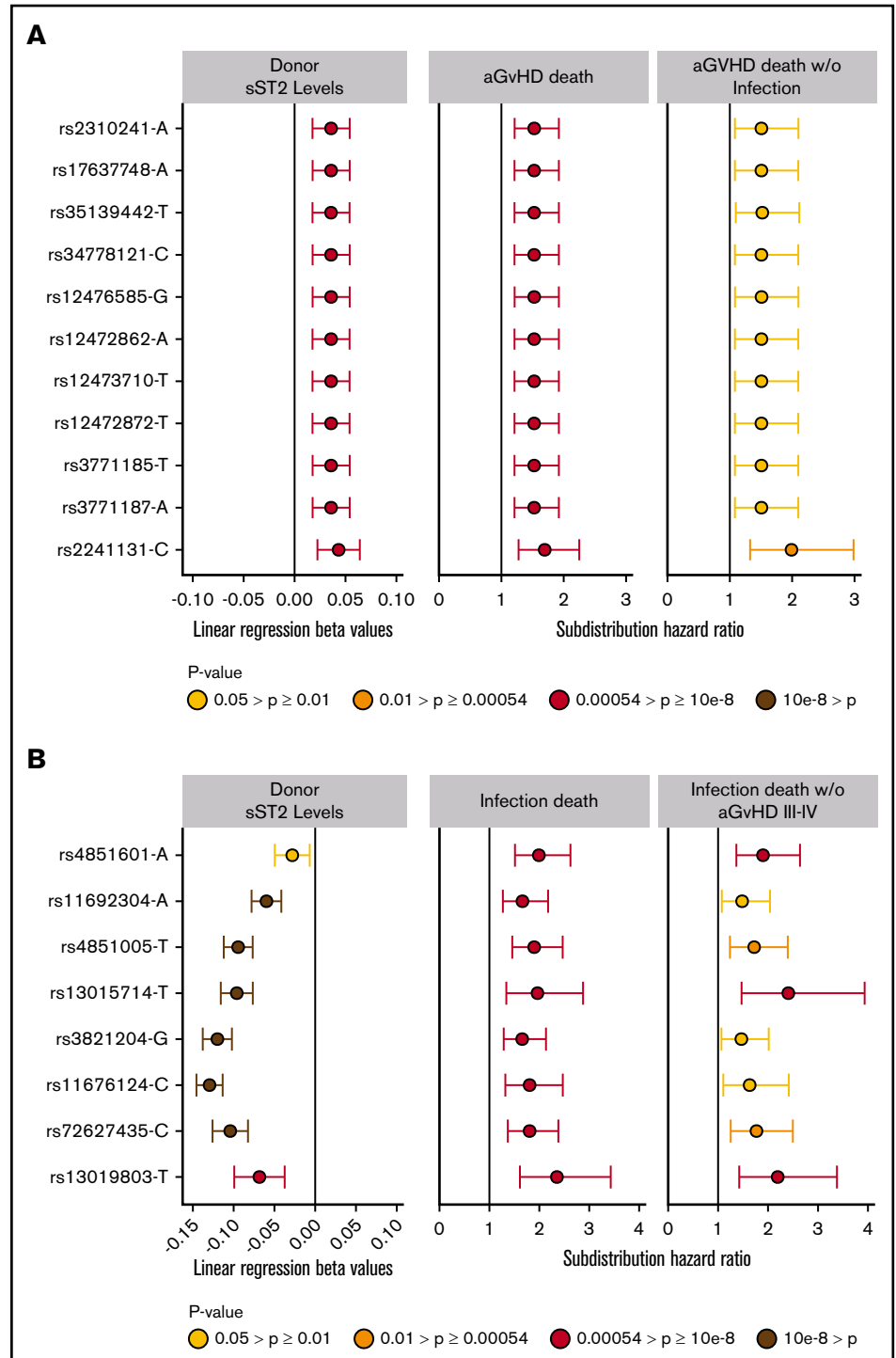
Figure 2. Regional association plot showing donor SNP associations with sST2 concentrations in plasma and serum and LD structure of the *IL1RL1* region.

(A) Genomic positions of SNPs are shown in mega-bases on the x-axis with mapped genes labeled by their HGNC symbols. $-\log_{10} P$ values obtained from linear regression models of donor SNPs on log-transformed sST2 concentrations in serum and plasma are shown on the left y-axis. The shape of the data point indicates the regulatory effect of the SNP; line color of the shape denotes associations from previous studies, where blue and green show genome-wide association with a trait and multiple effects (GWAS hit or association with gene expression or methylation levels), respectively. These colors indicate that a majority of the associated SNPs showed a direct regulatory effect on a transcript, indicating the denoted region contained multiple eQTL. Fill color for each SNP indicates the r^2 with the sentinel SNP, rs950880 (our most significant SNP-sST2 association), shown in a yellow-red gradient, with yellow indicating low LD ($r^2 < 0.2$) and red, high LD ($r^2 > 0.8$). Blue line coupled with the right y-axis shows the recombination rate in centi-Morgan (cM) per megabase. (B) Pairwise-LD heatmap of the region showing pairwise r^2 between SNPs. Brighter red indicates stronger correlation between SNP pairs.

with which promoter fragments interact are captured and sequenced. These paired pieces are then tested for statistical significance to identify PIRs.^{20,24} PIRs are important, as

variation in these regions can be connected to potential gene targets and may thus affect gene function.²³ To determine if significant variants were in PIRs, SNP positions for associated

Figure 3. Significant sST2-donor SNP association β values and hazard ratios for aGVHD death and infection death. Plots show the relationship of donor SNPs with sST2 levels in donors and death from aGVHD death (A) and infection (B). SNPs are shown in the y-axis with rs identification (ID) and the effect allele, in order by chromosome position. The point colors indicate the P values of the SNP for each analysis. Only SNPs that pass multiple test correction are included in the panel. The left column shows the coefficient β values with confidence intervals (CIs) of donor SNP associations with sST2 plasma/serum levels. The middle column shows sub-distribution hazard ratios and CIs from competing risk models with aGVHD death as primary cause. The right column shows results from competing risk models of aGVHD death as the primary cause without infection. (B) The left panel shows the coefficient β values with CIs of donor SNP associations with sST2 plasma/serum levels. The middle panel shows sub-distribution hazard ratios from a cox proportional model and competing risk model (HRs) and CIs of competing risk models with death caused by infection. The right column shows results from competing risk models with death due to infection among patients who did not experience aGVHD III-IV.



variants were superimposed on a map of significant bait-target pairs in the GM12878 cell line.^{22,42}

Results

Patient and donor characteristics

Patient and donor characteristics are shown in Table 1. AML and MDS proportions and donor age and graft source differed between cohorts ($P < .001$). The study design is shown in Figure 1.

SNP-sST2 plasma and serum concentration associations

We tested the associations of donor SNPs selected from the 1-Mb region around *IL1RL1* with donor sST2 concentrations. In total, 1265 donor SNPs were associated at $P < .05$ with donor sST2 serum/plasma concentrations, represented by 93 independent variants ($r^2 = 0.60$ and MAF = 0.05; Figures 1 and 2). Recipient SNP association with sST2 serum/plasma concentrations showed

664 SNPs at $P < .05$, represented by 11 independent variants (supplemental Table 1). All donor and recipient SNPs that were associated with sST2 levels at $P < .05$ replicated in same direction of effect as seen in the genomic atlas of human plasma proteome.¹³ Effect sizes of recipient SNP associations with sST2 levels were smaller with larger standard errors than donor SNP-sST2 associations. These 1265 donor SNPs were then tested for association with recipient death due to aGVHD and infection by using competing risk models (Figure 1). Although the recipient SNP-sST2 associations were less compelling, for comprehensiveness, these 1265 SNPs were also tested for association in the recipient population.

SNP associations with death due to aGVHD

There were 95 aGVHD primary-cause deaths in cohort 1 and 56 in cohort 2 (Table 1).²⁹ Multivariate aGVHD competing risk models constructed using AIC included AML diagnosis, recipient obesity ($>30 \text{ mg/kg}^2$), peripheral blood cell source, and donor age. No other variables were selected for inclusion in the model (supplemental Table 2).

Meta-analysis of competing risk results from cohorts 1 and 2 for all 1265 donor sST2-associated SNPs with aGVHD death are shown in supplemental Table 3. Correction for 93 independent variants yielded a significant $P < 5.4 \times 10^{-4}$; all variants with P less than this value were considered significant. We identified 11 aGVHD death-associated SNPs (Figure 3A). Stepwise competing risk analyses identified rs2310241 and rs2241131 (Table 2). The risk alleles at rs2310241-A and rs2241131-C correlated with higher levels of sST2 ($P = 1.3 \times 10^{-4}$ and $P = 5.0 \times 10^{-5}$, respectively) and increased risk of aGVHD death (HR = 1.5; $P_{\text{meta}} = 3.3 \times 10^{-4}$, and HR = 1.7; $P_{\text{meta}} = 2.6 \times 10^{-4}$, respectively), for each additional donor risk allele (supplemental Table 3). There was no evidence of heterogeneity of effect between cohorts. To assess the robustness of the association, we excluded patients with infection as a secondary cause of death (~38% of all aGVHD primary deaths); the results remained consistent after excluding these patients (Figure 3A). The SNPs correlated modestly ($r^2 = 0.52$), and the AIC including both variants was approximately equivalent to those of the single SNP models; thus, no additional information was gained from including both SNPs in a multiallele model. Cumulative incidence curves for rs2310241 and rs2241131 are shown in Figure 4. None of the significant aGVHD SNPs were associated with the competing risk model of TRM or the Cox proportional hazards models of OS.

No recipient SNPs were associated with aGVHD death. rs3917290, the most significant recipient SNP associated with aGVHD death in cohorts 1 ($P = .015$) and 2 ($P = .17$), were not associated with sST2 at $P < .05$.

sST2-SNP associations with death caused by infection

There were 86 and 25 deaths in which infection was the primary cause in cohorts 1 and 2, respectively (Table 1).²⁹ In 92% of cases, infection deaths were confirmed by a culture or biopsy of the organism, and almost one-third of the patients had autopsy records available for review, confirming infection as the cause of death.²⁹ Causes of infection death and affected organs are shown in supplemental Figure 1A-B. Multivariate clinical models of infection death, constructed using AIC, included recipient age,

Table 2. Independent significant SNP associations with GVHD death and infection deaths

Primary cause of death/SNP	SNP position on chr 2 (hg19)	Allele (ref/risk)	Risk allele frequency (C1/C2)	Cohort 1		Cohort 2		Meta analyses of cohorts 1 and 2	
				HR (95% CI)	P	HR (95% CI)	P	HR (95% CI)	P
GVHD									
rs2241131*	102804041	A/C	0.69/0.72	1.46 (1.05-2.02)	.024	2.71 (1.53-4.82)	6.7×10^{-4}	1.69 (1.28-2.25)	2.6×10^{-4}
rs2310241*	102841949	C/A	0.51/0.54	1.37 (1.01-1.84)	.04	1.81 (1.25-2.62)	1.6×10^{-3}	1.53 (1.21-1.92)	3.3×10^{-4}
Infection									
rs11676124*	102941338	T/C	0.62/0.61	1.7 (1.2-2.4)	3×10^{-3}	2.39 (1.15-4.99)	.02	1.81 (1.32-2.47)	2.2×10^{-4}
rs11692304	103095404	G/A	0.47/0.48	1.61 (1.19-2.16)	2×10^{-3}	1.95 (1.03-3.7)	.041	1.66 (1.27-2.18)	2.2×10^{-4}
rs13015714	102971865	G/T	0.77/0.76	1.79 (1.17-2.79)	8×10^{-3}	2.92 (1.22-6.97)	.016	1.96 (1.34-2.88)	5.3×10^{-4}
rs72627435*	102897739	T/C	0.21/0.20	1.76 (1.29-2.4)	3.8×10^{-4}	2.01 (1.09-3.69)	.024	1.81 (1.37-2.38)	2.8×10^{-5}
rs4851005	103011552	C/T	0.37/0.34	1.85 (1.38-2.47)	3.3×10^{-5}	2.17 (1.15-4.09)	.017	1.9 (1.46-2.47)	1.9×10^{-6}
rs13019803	102776202	C/T	0.08/0.08	2.31 (1.51-3.63)	1.1×10^{-4}	2.53 (1.11-5.77)	.028	2.35 (1.61-3.43)	8.9×10^{-6}
rs4851601*	103116261	G/A	0.28/0.26	2.01 (1.48-2.79)	8.3×10^{-6}	1.92 (1.03-3.6)	.042	1.99 (1.51-2.62)	9.7×10^{-7}
Multiallele	—	GCG/TTA		1.94 (1.54-2.44)	1.8×10^{-8}	2.24 (1.36-3.69)	.002	1.99 (1.61-2.45)	1.2×10^{-10}

SNP associations with GVHD death are adjusted for AML diagnosis, recipient obesity ($>30 \text{ mg/kg}^2$), donor age, and peripheral blood cell source. SNP associations with infection death are adjusted for recipient age, advanced disease at HCT, and recipient and donor CMV status. For infection, we computed a multiallele model that included the clinical covariates plus a variable collapsing the SNPs shown in bold, such that recipients have between 0 and 6 donor risk alleles. For GVHD, SNPs showed some LD ($r^2 = 0.52$) and were thus better markers alone than collectively. Cohort 1 (C1), n = 1584; cohort 2 (C2), n = 669. hg19, position according to human reference genome version hg19; Ref, reference allele; Risk, risk allele. *SNP is imputed.

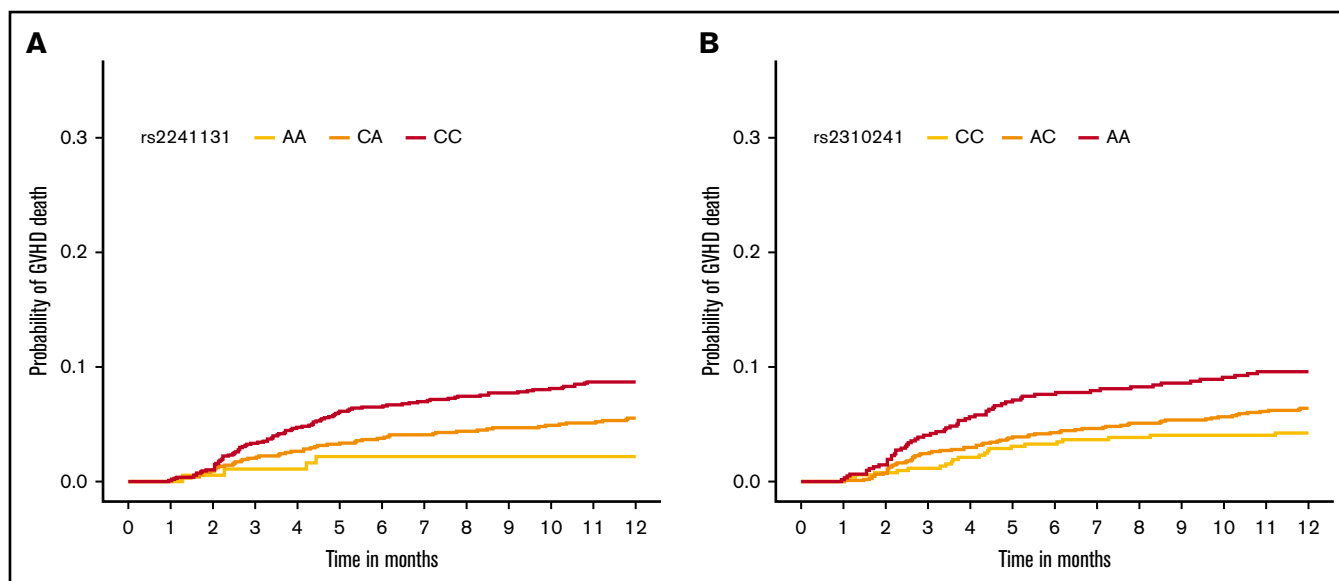


Figure 4. Cumulative incidence function of aGVHD death, according to donor SNP. The cumulative incidence of aGVHD death in the first year after HCT by rs2241131 (A) and rs2310241 (B) genotypes.

advanced disease at HCT, donor⁺/recipient⁻ CMV status, and peripheral blood cell source (supplemental Table 2). Results of competing risk models of infection death, including clinical variables, and each of the 1265 donor SNPs are shown in supplemental Table 4. Upon multiple-test correction, 7 independent SNPs were found to be associated with infection death (Table 2). There was no evidence of heterogeneity of effect between cohorts, and thus random-effects models were not used.

The final model included recipient age, advanced disease at HCT, donor⁺/recipient⁻ CMV status, peripheral blood cell source, rs4851601 ($P_{\text{meta}} = 9.7 \times 10^{-7}$), rs13019803 ($P_{\text{meta}} = 8.9 \times 10^{-6}$), and rs13015714 ($P_{\text{meta}} = 5.3 \times 10^{-4}$), with risk alleles at each SNP increasing risk of infection death approximately twofold. Figure 3B shows the associated donor alleles at each SNP associated with lower donor sST2 levels at rs4851601 ($P = .01$), rs13019803 ($P = 1.6 \times 10^{-5}$), and rs13015714 (1.2×10^{-20}). To assess the robustness of the association of the infection risk variants, we excluded patients with aGVHD III-IV (29% of all deaths from primary infection), and the results remained consistent after the patients were excluded (Figure 3B).

The multiallele model with rs4851601, rs13019803, and rs13015714 showed an increased risk of infection death of ~2- and 2.25-fold in cohorts 1 ($P = 1.8 \times 10^{-8}$) and 2 ($P = .002$), respectively (Table 2; Figure 5). The risk allele T in rs13019803 translated to an increased risk of TRM ($\text{HR}_{\text{meta}} = 1.51$; 95% meta CI [CI_{meta}] 1.21-1.88; $P_{\text{meta}} = 2.1 \times 10^{-4}$), but not OS ($\text{HR}_{\text{meta}} = 1.16$; 95% CI_{meta} [0.94-1.45]; $P_{\text{meta}} = .17$). The other infection risk variants were not associated with TRM or OS.

No recipient SNPs were associated with death due to infection after correction for multiple testing. rs1922296, the most significant recipient SNP associated with infection death in cohorts 1 ($P = .05$) and 2 ($P = .48$), was not associated with sST2 at $P < .05$ (data not shown).

Annotation of significantly associated variants

Annotation of donor SNPs associated with death due to aGVHD.

Data from the genomic atlas of human plasma proteome,¹³ corroborate the associations we identified between higher *IL1RL1* protein plasma levels and aGVHD death-risk alleles at rs2310241 and rs2241131. Although we did not measure *IL1R2* protein levels in DISCOVERY-BMT, the genomic atlas of the human plasma proteome¹³ showed that these risk alleles also correlate with increased *IL1R2* plasma protein levels ($P < 5 \times 10^{-6}$).¹³ Multiple databases showed that the risk allele at rs2310241 correlates with higher *IL18R1* expression in whole blood ($P = 1 \times 10^{-54}$), and both risk alleles at rs2310241 and rs2241131 significantly associate ($P < 5 \times 10^{-8}$) with increased *IL18RAP* expression in whole blood.^{18,43-46} Data extracted from the PhenoScanner database showed that the associated SNPs were adjacent to multiple GWAS SNPs (Figure 6A-B). In HSCs, B- and T-cells from the Epigenome Road Map dataset (supplemental Table 7), rs2310241 is located in or directly adjacent to (<900 base pairs) active enhancer regions, and rs2241131 resides in an upstream promoter region (Figure 6C-D). Furthermore, publicly available PChI-C data from the LCL show that rs2310141 also interacts with enhancers near *IL18RAP* and *IL1R2*. In the same LCL, both rs2310241 and rs2241131 reside in PChI-C target regions that interact with the promoters upstream of the transcription start site in *IL1RL2* and *MAP4K4* (supplemental Figure 2A-B; supplemental Table 5).

Annotation of donor SNPs associated with death due to infection.

Publicly available data in the genomic atlas of the human plasma proteome¹³ corroborate the associations we identified between lower *IL1RL1* protein plasma levels and infection death risk alleles at rs13015714 ($P = 2.1 \times 10^{-115}$), rs4851601 ($P = 2.1 \times 10^{-7}$), and rs13019803 ($P = 1.4 \times 10^{-28}$). Although we did not measure other proteins, the genomic atlas provided strong evidence that the T allele at rs13015714 is associated with decreased levels

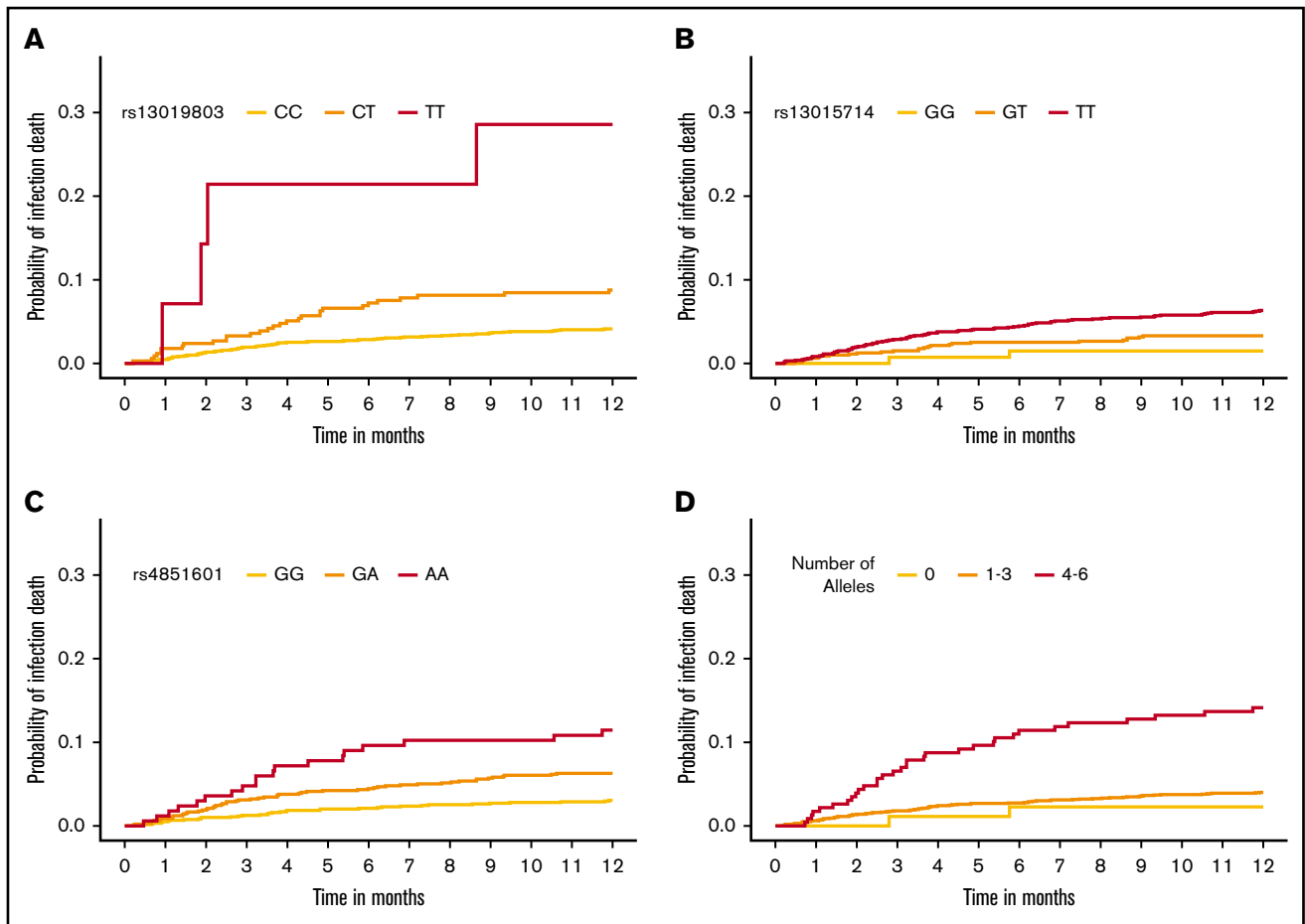


Figure 5. Cumulative incidence function of infection death, according to donor SNPs. The cumulative incidence of GVHD death in the first year after HCT by rs13019803 (A), rs13015714 (B), rs4851601 (C), and a multiallele model (D). (A-C) The multiallele model is the allele dosage sum of all 3 infection SNPs and was categorized for the number of total risk alleles: 0, 1 to 3, and 4 to 6, respectively.

of IL-18 receptor-1 protein, encoded by *IL18R1* ($\beta = -0.90 \pm 0.026$; $P = 1.3 \times 10^{-264}$). In addition, eQTLgen²⁸ data showed that increased gene expression of IL-18 receptor-associated protein (*IL18RAP*; $P = 3.3 \times 10^{-310}$) correlates with the rs13015714 T allele,¹³ and GTex data indicated that the T variant correlates with decreased expression of *IL1RL1* in lung ($\beta = -0.38 \pm 0.031$; $P = 4.0 \times 10^{-118}$).¹⁷ Data extracted from the PhenoScanner database¹⁹ showed that the infection death risk variants reside in a region with dozens of GWAS hits (Figure 6A) for multiple blood traits and inflammatory and autoimmune diseases (supplemental Table 6). The Epigenome Road Map showed rs13015714 is in the 3' end of *IL1RL1* and located in an upstream promoter across blood, HSC, T-cell and B-cell lines (Figure 5C; supplemental Table 7).¹⁸ Phi-C data from the LCL showed that all 3 infection-associated donor SNPs (rs13015714, rs4851601, and rs13019803), reside in target regions for enhancers near *IL18RAP* (supplemental Figure 3A-C; supplemental Table 5).⁴²

Discussion

Before HCT, identification of patients at risk of death associated with aGVHD or infection could alter approaches to GVHD and infection prophylaxis or donor selection. To date, individual SNP associations with aGVHD and infection death have not been successfully

replicated or validated, which is attributable to small sample sizes and the fact that a large majority of variants tested for association have been shown to have no biochemical function.³¹ A recent study using SNPs in cytokine genes constructed high- and low-risk groups for acute GVHD incidence; however, predictive genetic models were not significant for nonrelapse mortality.⁴⁷ By leveraging the large sample size and relatively homogenous independent cohorts of DISCOVeRY-BMT, we are uniquely placed to address this question and have adequate statistical power to test donor SNPs in this region for association with aGVHD or infection death.

We replicated the published sST2-SNP associations in DISCOVeRY-BMT HCT donors, and, in patients with AML or MDS, there was a correlation between sST2 levels and SNPs in the *IL1RL1* region, although the signal was muted. As expected, we demonstrated that alleles that correlated with high sST2 levels in donors correlated with death caused by aGVHD. In addition, both the aGVHD death risk loci, but not infection death loci, correlated with IL1R2 plasma protein levels.^{13,19} Higher IL1R2 protein levels have been shown to be robustly and significantly associated with GVHD mortality after transplantation into recipients, independent of sST2 associations, as shown in supplemental Table 8 in Vander Lugt et al.¹ This biomarker remains underexplored in patients and donors.

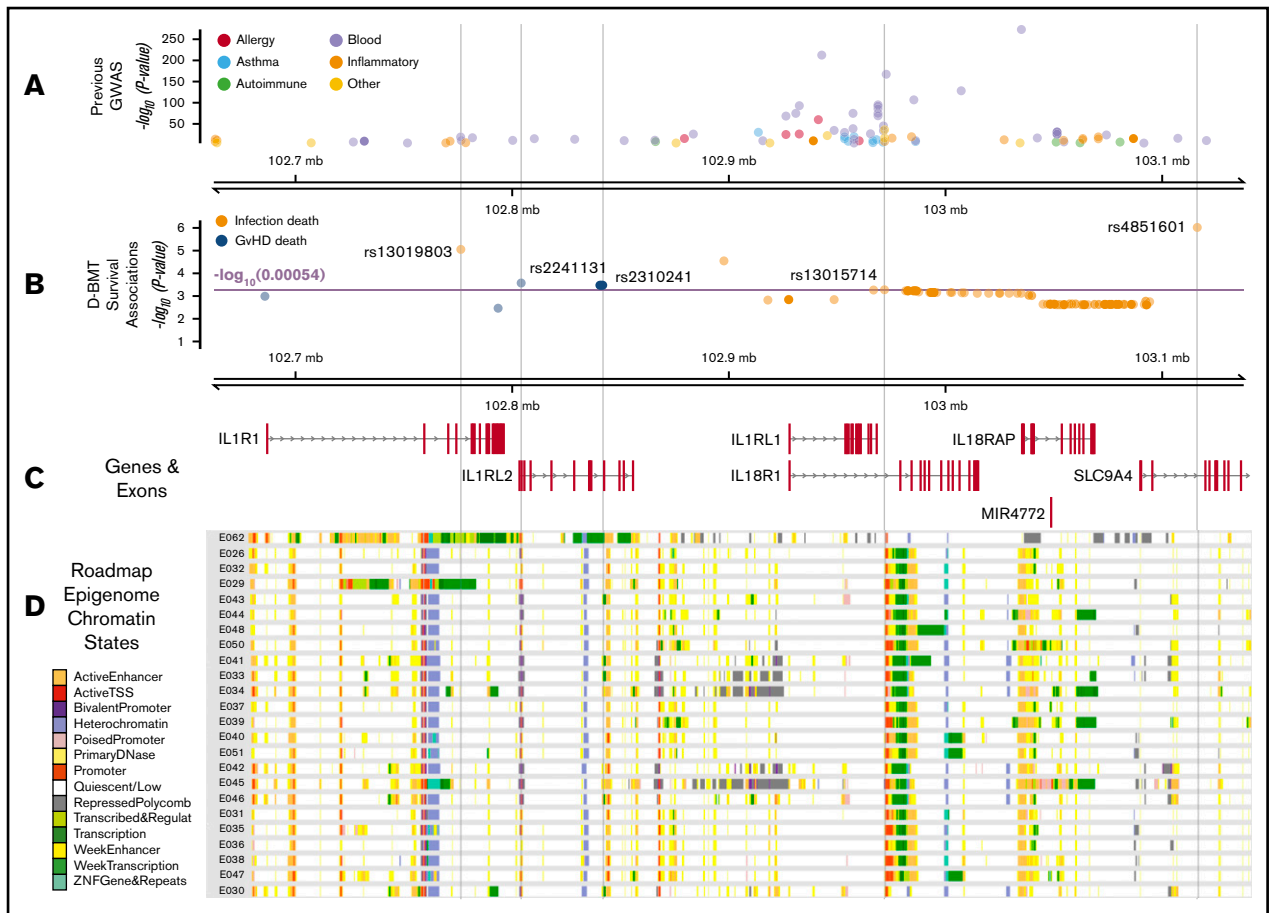


Figure 6. *IL1RL1* region with associated SNP *P* values annotated with previous GWAS and Roadmap Epigenome chromatin states. (A) GWAS SNPs in the *IL1RL1* region SNPs are classified by broad phenotypes indicated by the colored circles; all variants are associated at $P < 5 \times 10^{-8}$. (B) SNP associations in the *IL1RL1* region with infection death and aGVHD death at $P < .05$ in cohort 1 and replicated in cohort 2. All variants above the multiple test correction line (red) are considered significant. The x-axis is the chromosome position in megabase pairs and y-axis shows the $-\log_{10}(P \text{ values})$ for aGVHD and infection death. The higher the $-\log_{10}$ number, the lower the *P*. The SNPs selected using step-AIC for multi-allele models, for death from aGVHD (rs2241131 and rs2310241), and infection (rs4851601, rs13019803 and rs13015714) are highlighted with dashed lines drawn through the point to show the relationship of the variant to GWAS hits and epigenome road map data. (C) Genes in the region were mapped from UCSC build hg19, based on the known Gene Track (C) and annotated with chromatin states from Roadmap Epigenome project (D) for all blood, T cells, HSCs and B cells. The cell line numbers shown down the left side correspond to specific Roadmap Epigenome cell line identifiers (supplemental Table 7). The colors indicate ChromHmm status which is shown in the key.

IL1RL1 donor alleles associated with low sST2 levels were significantly associated with recipient risk of death from infection. For the donor T allele in rs1308491, linked with both low donor sST2 and significant hazard of recipient infection death, this association was strong enough to translate to an increased hazard of TRM. Our novel finding in DISCOVERy-BMT that low sST2 levels correlate with a poor health outcome (death due to infection) is not without precedent; the T allele in rs13019803 has been shown in a large heart health study to correlate with higher mortality.¹¹ Alleles of the SNPs that show an increased risk of infection death have consistently been shown to reduce the risk of inflammatory diseases, such as asthma, atopic dermatitis, celiac disease, Crohn's disease, and IBD. For example, the T allele at rs13015714 is in perfect linkage disequilibrium (LD; $r^2 = 1$) with the C allele of rs2001461, shown to be inversely associated with genome-wide significant risk of atopic dermatitis, celiac disease, Crohn's disease, and IBD.^{25,48-53} In addition, variants in LD ($r^2 = 1$) with rs13015714 are shown to be enriched in

the transcription factor T-bet, which specifies Th1 lineage and represses alternative T-cell fates.⁵⁴ Together, ChIP-seq and *IL18RAP* gene expression data indicate that the T allele at rs13015714 has increased T-bet binding and *IL18RAP* expression.⁵⁴ Our risk variant thus alters the binding of a lineage-specific transcription factor and gene expression of one of the genes (*IL18RAP*) that forms the IL-18 receptor; IL-18 synergizes with IL-12 to induce interferon- γ .⁵⁴

Immune response can act as a double-edged sword, where attenuated response can lead to infection and too strong a response can cause deleterious inflammation.⁵⁵ Because many cellular mechanisms and pathways overlap between infection defense and inflammation, it may be plausible to think that variants that render healthy donors more susceptible to inflammation (ie, the T allele at rs13015714) would actually protect immunosuppressed patients from infection. In other words, donors with these genetic variants would have a higher probability of having a more "reactive" immune system, which would help patients to fight infections better, once the donor cells are

grafted. This would also be consistent with the fact that, for example, the T allele of rs13015714 is significantly associated with increased lymphocyte count ($P = 1.7 \times 10^{-14}$), as shown in a 2016 paper in *Cell* that captured allelic associations with blood cell traits.²⁸ Therefore, lower levels of an inflammatory marker like sST2 in donors could suggest that donor cells will be less likely to protect against infection in the patient. In addition, it is possible that the low sST2 and increased risk of an infection–death relationship may actually reflect what is occurring with membrane ST2 more than soluble ST2.

Indeed, in murine GVHD models, we have recently shown that sST2 is secreted by intestinal proinflammatory T cells during gut inflammation; conversely, protective ST2-expressing regulatory T cells are decreased.⁵⁶ High membrane ST2, equivalent to low sST2, may be anti-inflammatory, thereby limiting responses against pathogens. Mice are housed in conditions that prevent infection, but a murine model of low-sST2 infection-associated death is needed. This 1-Mb region plays an important role in the tuning of the immune response,¹³ and these variants are likely to partially dictate the fine balance between infection and inflammation.

The strengths of our study include a large, relatively homogeneous sample size; well-characterized survival outcomes; and the availability of both donor and recipient genotypes. In addition, the nonrisk alleles in 4 of the 5 aGVHD and infection death-associated variants are common (>5%) across multiple races and ethnicities, meaning that there is the potential for validating the DISCOVeRY-BMT findings in other populations. Despite the large sample size, the number of patients who died of infection was not large enough to allow us to investigate death due to specific infections, and patient death from aGVHD did not comprise a large portion of our patient population, thus reducing our power to detect smaller effect sizes. An additional limitation is the lack of longitudinal analyses; specifically, we did not measure the relationship of the donor genotype with recipient sST2 levels after transplantation.

Evidence from independent experiments showed that genetic variants in the *IL1RL1* region predicted IL1RL1 and IL1R2 protein levels, correlated with expression of multiple genes, and affected binding of important transcription factors. Data from our HCT donors corroborated the SNP association with sST2 levels and showed that these SNPs in the *IL1RL1* region correlated with increased risk of death from aGVHD or infection. Given further cell line experiments and replication in more diverse cohorts, these donor SNPs could be used in improved donor selection to help reduce the risk of such deaths in patients with AML or MDS who undergo HLA-matched unrelated HCT.

Acknowledgments

This work was supported by grants from the National Institutes of Health (NIH). Funding was provided by NIH, National Heart, Lung, and Blood Institute (NHLBI; 1R01HL102278); NIH, National Cancer Institute (NCI; 1R03CA188733) (L.E.S.-C. and T.E.H.); and a Pelotonia Foundation Graduate Student Fellowship (E.K.). Any opinions, findings, and conclusions expressed in this material are those of the authors and do not necessarily reflect those of the Pelotonia Fellowship Program or The Ohio State University. S.P. was supported by grants from NIH, NCI (R01CA168814), the National Institute of Child Health and Human Development (R01HD074587 and U54HD090215), and the Leukemia & Lymphoma Society

(1293-15). The CIBMTR is supported by Public Health Service Grant/Cooperative Agreement 5U24-CA076518 from the NCI, NHLBI, and the National Institute of Allergy and Infectious Diseases; Grant/Cooperative Agreement 5U10HL069294 from NHLBI and NCI; contract HHS250201200016C with Health Resources and Services Administration (HRSA/DHHS); and grants N00014-15-1-0848 and N00014-16-1-2020 from the Office of Naval Research. Further funding was received from Alexion; Amgen, Inc.; an anonymous donation to the Medical College of Wisconsin; Astellas Pharma US; AstraZeneca; Be the Match Foundation; Bluebird Bio, Inc.; Bristol Myers Squibb Oncology; Celgene Corporation; Cellular Dynamics International, Inc.; Chimerix, Inc.; Fred Hutchinson Cancer Research Center; Gamida Cell, Ltd.; Genentech, Inc.; Genzyme Corporation; Gilead Sciences, Inc.; Health Research, Inc.; Roswell Park Cancer Institute; HistoGenetics, Inc.; Incyte Corporation; Janssen Scientific Affairs, LLC; Jazz Pharmaceuticals, Inc.; Jeff Gordon Children's Foundation; The Leukemia & Lymphoma Society; Medac, GmbH; MedImmune; The Medical College of Wisconsin; Merck & Co, Inc.; Mesoblast; MesoScale Diagnostics, Inc.; Miltenyi Biotec, Inc.; National Marrow Donor Program; Neovii Biotech NA, Inc.; Novartis Pharmaceuticals Corporation; Onyx Pharmaceuticals; Optum Healthcare Solutions, Inc.; Otsuka America Pharmaceutical, Inc.; Otsuka Pharmaceutical Co, Ltd., Japan; Patient-Centered Outcomes Research Institute; Perkin Elmer, Inc.; Pfizer, Inc.; Sanofi US; Seattle Genetics; Spectrum Pharmaceuticals, Inc.; St. Baldrick's Foundation; Sunesis Pharmaceuticals, Inc.; Swedish Orphan Biovitrum, Inc.; Takeda Oncology; Telomere Diagnostics, Inc.; University of Minnesota; and Wellpoint, Inc.

The views expressed in this article do not reflect the official policy or position of the National Institutes of Health, the Department of the Navy, the Department of Defense, Health Resources and Services Administration or any other agency of the US Government.

Authorship

Contribution: E.K., S.P., and L.E.S.-C. designed and performed the research and analysis and wrote the manuscript; S.P. and A.J.D. measured the ST2 levels; E.K., J.W., A.A.R., L.E.S.-C., and L. Preus analyzed the data and generated the figures; C.A.H., D.S., L. Pooler, L. Preus, S.L., L.Y., Q.L., Q.Z., M.D.H., T.W., A.W., and G.B. performed genotyping, imputation and/or data quality control; T.H. helped design the research, interpreted the results, and edited the paper; P.L.M., M.C.P., S.J.L., and S.R.S. interpreted the results and edited the paper; and all authors reviewed and approved the manuscript.

Conflict-of-interest disclosure: S.P. holds the patent, "Methods of detection of graft-versus-host disease" (US 20130115232A1, WO2013066369A3), licensed to Viracor-IBT Laboratories. The remaining authors declare no competing financial interests.

ORCID profiles: E.K., 0000-0002-0881-7424; A.J.D., 0000-0002-1401-9744; Q.Z., 0000-0003-2516-6675; D.S., 0000-0001-7099-9022; L. Pooler, 0000-0001-5388-6640; X.S., 0000-0002-6844-2740; P.L.M., 0000-0002-9577-3879; S.J.L., 0000-0003-2600-6390; S.P., 0000-0001-5571-2775.

Correspondence: Lara E. Sucheston-Campbell, The Ohio State University, 604 Riffe Building, 496 W 12th Ave, Columbus, OH 43210; e-mail: sucheston-campbell.1@osu.edu; and Sophie Paczesny, Indiana University School of Medicine, 1044 W Walnut St, Room 425, Indianapolis, IN 46202; e-mail: sophpacz@iu.edu.

References

1. Vander Lugt MT, Braun TM, Hanash S, et al. ST2 as a marker for risk of therapy-resistant graft-versus-host disease and death. *N Engl J Med*. 2013;369(6):529-539.
2. Ponce DM, Hilden P, Mumaw C, et al. High day 28 ST2 levels predict for acute graft-versus-host disease and transplant-related mortality after cord blood transplantation. *Blood*. 2015;125(1):199-205.
3. McDonald GB, Tabellini L, Storer BE, Lawler RL, Martin PJ, Hansen JA. Plasma biomarkers of acute GVHD and nonrelapse mortality: predictive value of measurements before GVHD onset and treatment. *Blood*. 2015;126(1):113-120.
4. Levine JE, Braun TM, Harris AC, et al; Blood and Marrow Transplant Clinical Trials Network. A prognostic score for acute graft-versus-host disease based on biomarkers: a multicentre study. *Lancet Haematol*. 2015;2(1):e21-e29.
5. Yu J, Storer BE, Kushekhar K, et al. Biomarker Panel for Chronic Graft-Versus-Host Disease. *J Clin Oncol*. 2016;34(22):2583-2590.
6. Abu Zaid M, Wu J, Wu C, et al. Plasma biomarkers of risk for death in a multicenter phase 3 trial with uniform transplant characteristics post-allogeneic HCT. *Blood*. 2017;129(2):162-170.
7. Hartwell MJ, Özbek U, Holler E, et al. An early-biomarker algorithm predicts lethal graft-versus-host disease and survival. *JCI Insight*. 2017;2(3):e89798.
8. Kanakry CG, Bakoyannis G, Perkins SM, et al. Plasma-derived proteomic biomarkers in HLA-haploidentical or HLA-matched bone marrow transplantation using post-transplantation cyclophosphamide. *Haematologica*. 2017;102(5):932-940.
9. Pascual-Figal DA, Januzzi JL. The biology of ST2: the International ST2 Consensus Panel. *Am J Cardiol*. 2015;115:3B-7B.
10. Griesenauer B, Paczesny S. The ST2/IL-33 Axis in Immune Cells during Inflammatory Diseases. *Front Immunol*. 2017;8:475.
11. Ho JE, Chen WY, Chen MH, et al; CARDIoGRAM Consortium; CHARGE Inflammation Working Group; CHARGE Heart Failure Working Group. Common genetic variation at the IL1RL1 locus regulates IL-33/ST2 signaling. *J Clin Invest*. 2013;123(10):4208-4218.
12. Yao C, Chen G, Song C, et al. Genome-wide mapping of plasma protein QTLs identifies putatively causal genes and pathways for cardiovascular disease. *Nat Commun*. 2018;9(1):3268.
13. Sun BB, Maranville JC, Peters JE, et al. Genomic atlas of the human plasma proteome. *Nature*. 2018;558(7708):73-79.
14. Folkersen L, Fauman E, Sabater-Lleal M, et al; IMPROVE study group. Mapping of 79 loci for 83 plasma protein biomarkers in cardiovascular disease. *PLoS Genet*. 2017;13(4):e1006706.
15. Suhre K, Arnold M, Bhagwat AM, et al. Connecting genetic risk to disease end points through the human blood plasma proteome. *Nat Commun*. 2017;8:14357.
16. Lourdasamy A, Newhouse S, Lunnon K, et al; AddNeuroMed Consortium; Alzheimer's Disease Neuroimaging Initiative. Identification of cis-regulatory variation influencing protein abundance levels in human plasma. *Hum Mol Genet*. 2012;21(16):3719-3726.
17. Consortium G; GTEx Consortium. The Genotype-Tissue Expression (GTEx) project. *Nat Genet*. 2013;45(6):580-585.
18. Ward LD, Kellis M. HaploReg v4: systematic mining of putative causal variants, cell types, regulators and target genes for human complex traits and disease. *Nucleic Acids Res*. 2016;44:D877-D881.
19. Staley JR, Blackshaw J, Kamat MA, et al. PhenoScanner: a database of human genotype-phenotype associations. *Bioinformatics*. 2016;32(20):3207-3209.
20. Schoenfelder S, Javierre BM, Furlan-Magaril M, Wingett SW, Fraser P. Promoter Capture Hi-C: High-resolution, Genome-wide Profiling of Promoter Interactions. *J Vis Exp*. 2018;(136):
21. Javierre BM, Burren OS, Wilder SP, et al; BLUEPRINT Consortium. Lineage-Specific Genome Architecture Links Enhancers and Non-coding Disease Variants to Target Gene Promoters. *Cell*. 2016;167(5):1369-1384.e19.
22. Mifsud B, Tavares-Cadete F, Young AN, et al. Mapping long-range promoter contacts in human cells with high-resolution capture Hi-C. *Nat Genet*. 2015;47(6):598-606.
23. Spurrell CH, Dickel DE, Visel A. The Ties That Bind: Mapping the Dynamic Enhancer-Promoter Interactome. *Cell*. 2016;167(5):1163-1166.
24. Cairns J, Freire-Pritchett P, Wingett SW, et al. CHICAGO: robust detection of DNA looping interactions in Capture Hi-C data. *Genome Biol*. 2016;17(1):127.
25. Festen EA, Goyette P, Green T, et al. A meta-analysis of genome-wide association scans identifies IL18RAP, PTPN2, TAGAP, and PUS10 as shared risk loci for Crohn's disease and celiac disease. *PLoS Genet*. 2011;7(1):e1001283.
26. Xia Y, Liu YQ, Chen K, Wang LC, Ma CY, Zhao YR. Association of IL-1R2 genetic polymorphisms with the susceptibility of ankylosing spondylitis in Northern Chinese Han population. *Mod Rheumatol*. 2015;25(6):908-912.
27. Casper J, Zweig AS, Villarreal C, et al. The UCSC Genome Browser database: 2018 update. *Nucleic Acids Res*. 2018;46(D1):D762-D769.
28. Astle WJ, Elding H, Jiang T, et al. The Allelic Landscape of Human Blood Cell Trait Variation and Links to Common Complex Disease. *Cell*. 2016;167(5):1415-1429.e19.
29. Hahn T, Sucheston-Campbell LE, Preus L, et al. Establishment of Definitions and Review Process for Consistent Adjudication of Cause-specific Mortality after Allogeneic Unrelated-donor Hematopoietic Cell Transplantation. *Biol Blood Marrow Transplant*. 2015;21(9):1679-1686.
30. Clay-Gilmour AI, Hahn T, Preus LM, et al. Genetic association with B-cell acute lymphoblastic leukemia in allogeneic transplant patients differs by age and sex. *Blood Adv*. 2017;1(20):1717-1728.

31. Karaesmen E, Rizvi AA, Preus LM, et al. Replication and validation of genetic polymorphisms associated with survival after allogeneic blood or marrow transplant. *Blood*. 2017;130(13):1585-1596.
32. Zhu Q, Yan L, Liu Q, et al. Exome chip analyses identify genes affecting mortality after HLA-matched unrelated-donor blood and marrow transplantation. *Blood*. 2018;131(22):2490-2499.
33. Yan L, Ma C, Wang D, et al. OSAT: a tool for sample-to-batch allocations in genomics experiments. *BMC Genomics*. 2012;13:689.
34. R Core Team. R: A language and environment for statistical computing. Vienna, Austria: R Foundation for Statistical Computing. <https://www.R-project.org/>. Accessed 2 July 2018.
35. Arnold M, Raffler J, Pfeufer A, Suhre K, Kastenmüller G. SNIIPA: an interactive, genetic variant-centered annotation browser. *Bioinformatics*. 2015;31(8):1334-1336.
36. Fine JP, Gray RJ. A Proportional Hazards Model for the Subdistribution of a Competing Risk. *J Am Stat Assoc*. 1999;94(446):496-509.
37. Kuk D, Varadhan R. Model selection in competing risks regression. *Stat Med*. 2013;32(18):3077-3088.
38. Viechtbauer W. Conducting Meta-Analyses in R with the metafor Package. *J Stat Softw*. 2010;36(3):11-15.
39. Hendricks AE, Dupuis J, Logue MW, Myers RH, Lunetta KL. Correction for multiple testing in a gene region. *Eur J Hum Genet*. 2014;22(3):414-418.
40. Kundaje A, Meuleman W, Ernst J, et al; Roadmap Epigenomics Consortium. Integrative analysis of 111 reference human epigenomes. *Nature*. 2015;518(7539):317-330.
41. Hahne F, Ivanek R. Visualizing Genomic Data Using Gviz and Bioconductor. *Methods Mol Biol*. 2016;1418:335-351.
42. Schofield EC, Carver T, Achuthan P, et al. CHiCP: a web-based tool for the integrative and interactive visualization of promoter capture Hi-C datasets. *Bioinformatics*. 2016;32(16):2511-2513.
43. Consortium EP; ENCODE Project Consortium. An integrated encyclopedia of DNA elements in the human genome. *Nature*. 2012;489(7414):57-74.
44. Westra HJ, Peters MJ, Esko T, et al. Systematic identification of trans eQTLs as putative drivers of known disease associations. *Nat Genet*. 2013;45(10):1238-1243.
45. Zhernakova DV, Deelen P, Vermaat M, et al. Identification of context-dependent expression quantitative trait loci in whole blood. *Nat Genet*. 2017;49(1):139-145.
46. Joehanes R, Zhang X, Huan T, et al. Integrated genome-wide analysis of expression quantitative trait loci aids interpretation of genomic association studies. *Genome Biol*. 2017;18(1):16.
47. Martínez-Laperche C, Buces E, Aguilera-Morillo MC, et al; GVHD/Immunotherapy Committee of the Spanish Group for Hematopoietic Transplantation. A novel predictive approach for GVHD after allogeneic SCT based on clinical variables and cytokine gene polymorphisms. *Blood Adv*. 2018;2(14):1719-1737.
48. Paternoster L, Standl M, Waage J, et al; Australian Asthma Genetics Consortium (AAGC). Multi-ancestry genome-wide association study of 21,000 cases and 95,000 controls identifies new risk loci for atopic dermatitis. *Nat Genet*. 2015;47(12):1449-1456.
49. Hirota T, Takahashi A, Kubo M, et al. Genome-wide association study identifies eight new susceptibility loci for atopic dermatitis in the Japanese population. *Nat Genet*. 2012;44(11):1222-1226.
50. Dubois PC, Trynka G, Franke L, et al. Multiple common variants for celiac disease influencing immune gene expression. *Nat Genet*. 2010;42(4):295-302.
51. Hunt KA, Zhernakova A, Turner G, et al. Newly identified genetic risk variants for celiac disease related to the immune response. *Nat Genet*. 2008;40(4):395-402.
52. Jostins L, Ripke S, Weersma RK, et al; International IBD Genetics Consortium (IIBDGC). Host-microbe interactions have shaped the genetic architecture of inflammatory bowel disease. *Nature*. 2012;491(7422):119-124.
53. Liu JZ, van Sommeren S, Huang H, et al; International Multiple Sclerosis Genetics Consortium; International IBD Genetics Consortium. Association analyses identify 38 susceptibility loci for inflammatory bowel disease and highlight shared genetic risk across populations. *Nat Genet*. 2015;47(9):979-986.
54. Soderquest K, Hertweck A, Giambartolomei C, et al. Genetic variants alter T-bet binding and gene expression in mucosal inflammatory disease. *PLoS Genet*. 2017;13(2):e1006587.
55. Si-Tahar M, Touqui L, Chignard M. Innate immunity and inflammation--two facets of the same anti-infectious reaction. *Clin Exp Immunol*. 2009;156(2):194-198.
56. Zhang J, Ramadan AM, Griesenauer B, et al. ST2 blockade reduces sST2-producing T cells while maintaining protective mST2-expressing T cells during graft-versus-host disease. *Sci Transl Med*. 2015;7(308):308ra160.